Green Wireless Communications: A Time-Reversal Paradigm

Beibei Wang, *Member, IEEE,* Yongle Wu, Feng Han, *Student Member, IEEE,* Yu-Han Yang, *Student Member, IEEE,* and K. J. Ray Liu, *Fellow, IEEE*

***Abstract*—Green wireless communications have received considerable attention recently in hope of finding novel solutions to improve energy efficiency for the ubiquity of wireless applications. In this paper, we argue and show that the time-reversal (TR) signal transmission is an ideal paradigm for green wireless communications because of its inherent nature to fully harvest energy from the surrounding environment by exploiting the multi-path propagation to re-collect *all* the signal energy that would have otherwise been lost in most existing communication paradigms. A green wireless technology must ensure low energy consumption and low radio pollution to others than the intended user. In this paper, we show through theoretical analysis, numerical simulations and experiment measurements that the TR wireless communications, compared to the conventional direct transmission using a Rake receiver, reveals significant transmission power reduction, achieves high interference alleviation ratio, and exhibits large multi-path diversity gain. As such it is an ideal paradigm for the development of green wireless systems. The theoretical analysis and numerical simulations show an order of magnitude improvement in terms of transmit power reduction and interference alleviation. Experimental measurements in a typical indoor environment also demonstrate that the transmit power with TR based transmission can be as low as 20% of that without TR, and the average radio interference (thus radio pollution) even in a nearby area can be up to 6 dB lower. A strong time correlation is found to be maintained in the multi-path channel even when the environment is varying, which indicates high bandwidth efficiency can be achieved in TR radio communications.**

***Index Terms*—Green wireless communications, time reversal, energy efficiency, low radio pollution.**

I. Introduction

IN RECENT years, with the explosive growth of wireless communication industry in terms of network infrastructures, network users, and various new applications, the energy consumption of wireless networks and devices is experiencing a dramatic increase. Because of ubiquity of wireless applications, such an increasing energy consumption not only results in a high operational cost and an urgent demand for battery/energy capacity to wireless communications operators, but also causes a more severe electromagnetic (EM) pollution to the global environment. Therefore, an emerging concept of "Green Communications" has received considerable attention in hope of finding novel solutions to improve energy efficiency, relieve/reduce radio pollution to unintended users, and maintain/improve performance metrics.

Manuscript received 8 October 2010; revised 14 February 2011.

B. Wang and Y. Wu are with Qualcomm Inc., San Diego, CA 92121, USA (e-mail: {beibeiw, yonglew}@qualcomm.com).

F. Han, Y.-H. Yang, and K. J. R. Liu are with the Department of Electrical and Computer Engineering, University of Maryland, College Park, MD 20742, USA (e-mail: {hanf, yhyang, kjrliu}@umd.edu).

Digital Object Identifier 10.1109/JSAC.2011.110918.

In this paper, we argue and show that the time-reversal (TR) signal transmission is an ideal paradigm for green wireless communications because of its inherent nature to fully harvest energy from the surrounding environment by exploiting the multi-path propagation, as shown in Fig. 1, to re-collect *all* the signal energy that would have otherwise been lost in most existing communication paradigms. To qualify as a green wireless technology, one must meet two basic requirements: one is low energy consumption (environmental concerns) and the other is low radio pollution to others (health concerns) besides the intended transmitter and receiver. We will illustrate in this paper that the time-reversal paradigm not only meets the above two criteria but also exhibits a very high multi-path diversity gain, as well as preserving high bandwidth efficiency due to high channel correlation in practice.

TR wireless communication has been known for some time; however, its applications have been mainly considered as a specialty use for extreme multi-path environment. Therefore, not much development and interest can be seen beyond defense applications. The history of applying TR to communication systems dates back to early 1990's. In TR communications, when transceiver *A* wants to transmit information to transceiver *B*, transceiver *B* first has to send a delta-like pilot pulse that propagates through a scattering and multi-path environment and the signals are received by transceiver *A*; then, transceiver *A* simply transmits the time-reversed signals back through the same channel to transceiver *B*. By utilizing channel reciprocity, TR essentially leverages the multi-path channel as a matched filter, i.e., treats the environment as a facilitating matched filter computing machine, and focuses the wave at the receiver in both space and time domains. As such one can readily see the low-complexity nature of TR communications.

Experiments on TR in acoustics and ultrasound domains [1] [2] [3] [4] have shown that acoustic energy can be refocused on the source with very high resolution, and the focusing effect in real propagation environments was further validated by underwater acoustics experiments in the ocean [5] [6] [7]. Since TR can make full use of multi-path propagation and also requires no complicated channel measurements and estimation, it has been also studied in wireless communication systems. Spatial and temporal focusing properties of EM signal transmission with TR have been demonstrated in [8] [9] [10] by taking measurements in radio frequency (RF) communications. A TR-based interference canceller to mitigate the effect of clutter was presented in [11], and target detection in a highly cluttered environment using TR was investigated in [12] [13].

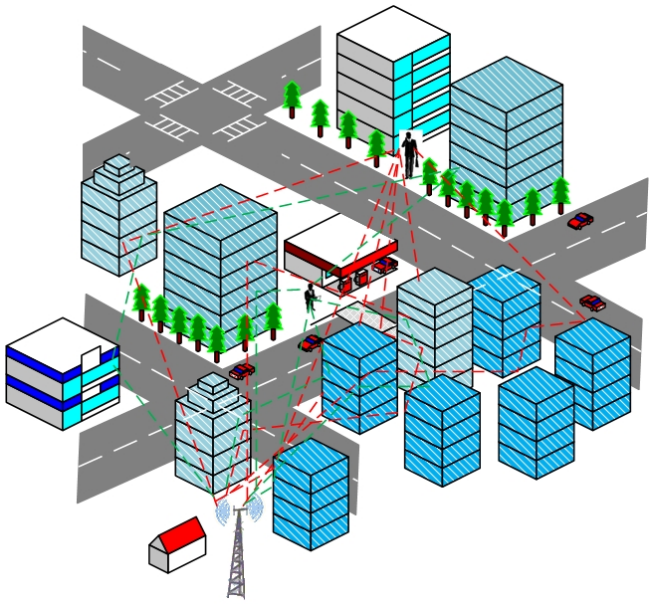

Fig. 1. Illustration of a typical urban multi-path environment.

Leveraging from the spatial and temporal focusing effect, in this paper, we show that the TR technique is indeed an ideal green wireless communication paradigm which can efficiently harvest energy from the environment. We first derive the theoretical transmission power reduction and interference alleviation of the TR-based transmission compared to direct transmission with a Rake receiver. Our theoretical analysis and simulations show that a potential of over an order of magnitude of power reduction and interference alleviation can be achieved. We also investigate the multi-path diversity gain of the TR-based transmission, in which we demonstrate a very high multi-path diversity gain exhibiting in a TR system. In essence, TR transmission treats each multi-path as a virtual antenna and makes full use of *all* the multi-paths.

Experimental results obtained from measurements in real RF multi-path environment are shown to demonstrate the great potential of TR-based transmission as an energy-efficient green wireless communication paradigm. It is found that in a typical indoor multi-path environment, in order to achieve the same receiver performance, TR-based transmission only costs as low as 20 % of the transmission power needed in direct transmission; moreover, the average interference can be up to 6 dB lower than that caused by direct transmission when the interfered receiver is only 1 m away from the intended receiver. It is also shown from channel measurements in different time epochs that, a static indoor multi-path environment is strongly time-correlated; therefore, there is no need for the receiver to keep sending pilot pulses to the transmitter, and the spectral efficiency can be much higher than typically achieved value of 50 %. We also performed extensive numerical simulation to validate the theoretical derivation.

The rest of this paper is organized as follows. In Section II, we introduce the system model and multi-path channel model. In Section III, we investigate the performance of the TR-based transmission in terms of power reduction, interference alleviation, and multi-path diversity gain. Simulation studies are presented in Section IV, and experimental results obtained from practical indoor multi-path channels are shown in Section V. We briefly present a few prospective applications of the TR-based technology based on its focusing effect in Section VI, which suggest that TR-based communication is a promising direction in addition to power efficiency and low interference pollution. Finally, conclusions are drawn in Section VII.

II. System Model

In this paper, we consider a slow fading wireless channel with a large delay spread. The channel impulse response (CIR) at time k between the transmitter and the receiver in discrete time domain is modeled as

$$h[k] = \sum_{l=0}^{L-1} h_l \delta[k-l], \tag{1}$$

where h_l is the complex amplitude of l-th tap of the CIR, and L is the number of channel taps. Since we assume that the channel is slow fading, the channel taps will not vary during the observation time. To gain some insight into the TR system while keeping the model analytically tractable, the CIRs associated with different receivers at different locations are assumed to be independent, e.g., when the receivers are very far apart. Furthermore, we assume independence among the taps of each CIR, i.e., the paths of each CIR are uncorrelated. Each $h[l]$ is a circular symmetric complex Gaussian (CSCG) random variable with zero mean and

$$E[|h[l]|^2] = e^{-\frac{lT_S}{\sigma_T}}, \tag{2}$$

where T_S is the sampling period of this system such that $1/T_S$ equals the system bandwidth B, and σ_T is the delay spread [14] of the channel.

A TR-based communication system is very simple. For example, a base station tries to transmit some information to an end user. Prior to the transmission, the end user has to send out a delta-like pilot pulse which propagates to the base station through a multi-path channel, where the base station keeps a record of the received waveform. Then, the base station time reverses the received waveform, and use the normalized time-reversed conjugate signals as a basic waveform, i.e.,

$$g[k] = h^*[L-1-k] \Big/ \sqrt{\sum_{l=0}^{L-1} |h[l]|^2}\ ,\ k = 0, 1, \ldots, L-1. \tag{3}$$

In the above equation, we ignore the noise term to simplify derivation[1]. Thanks to the channel reciprocity, the multi-path channel forms a *natural matched filter* to the basic waveform $g[k], k = 0, 1, \ldots, L-1$, and hence a peak is expected at the receiver.

The base station loads the data stream on the basic waveform, and transmits the signal into the wireless channel. Usually the baud rate is much lower than the sampling rate, and the ratio of the sampling rate to the baud rate is also known as the rate back-off factor D [10]. Mathematically, if a sequence of information symbols are denoted by $\{X[k]\}$ and assumed to be i.i.d. complex random variables with zero mean

[1]By sending a large number of channel training sequences from the receiver, the noise term is diminishing asymptotically.

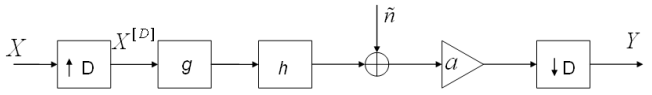

Fig. 2. The block diagram of a TR-based communication system.

and a variance of P, the transmitted signal into the wireless channels can be expressed as

$$S[k] = \left(X^{[D]} * g\right)[k], \tag{4}$$

where $X^{[D]}[k]$ is an up-sampled sequence of $X[k]$,

$$X^{[D]}[k] = \begin{cases} X[k/D], & \text{if } k \bmod D = 0, \\ 0, & \text{if } k \bmod D \neq 0. \end{cases} \tag{5}$$

The signal received at the receiver is the convolution of $\{S[k]\}$ and $\{h[k]\}$, plus additive white Gaussian noise (AWGN) $\{\tilde{n}_i[k]\}$ with zero-mean and variance σ^2. The receiver simply performs a one-tap gain adjustment to the received signal, i.e., multiplying a coefficient a, and then down-samples it with the same factor D. The signal before down-sampling can be represented as

$$Y^{[D]}[k] = a\left(X^{[D]} * g * h\right)[k] + a\tilde{n}[k]. \tag{6}$$

Accordingly, the down-sampled signal $Y[k]$ is as follows (for simplicity, $L-1$ is assumed to be a multiple of D)

$$Y[k] = a \sum_{l=0}^{(2L-2)/D} (h*g)[Dl]X[k-l] + an[k], \tag{7}$$

where

$$(h*g)[k] = \frac{\sum_{l=0}^{L-1} h[l]h^*[L-1-k+l]}{\sqrt{\sum_{l=0}^{L-1}|h[l]|^2}}, \tag{8}$$

with $k = 0, 1, \cdots, 2L-2$, and $n[k] = \tilde{n}[Dk]$, a white Gaussian additive noise with zero mean and variance σ^2. The block diagram of a TR-based communication system is summarized in Fig. 2, and we can see that both the transmitter and receiver are of very low complexity.

III. Performance Analysis

In this part, we compare the performance of the TR system to that of conventional direct transmission with Rake receivers, and evaluate several performance metrics, including the transmit power in order to achieve the same signal-to-interference-and-noise ratio (SINR), and the interference caused to unintended receivers. Finally, we analyze the multi-path gain of the TR system.

A. Power Reduction

Note that in (8), when $k = L-1$, it corresponds to the maximum-power central peak of the autocorrelation function of the CIR, i.e.

$$(h*g)[L-1] = \sqrt{\sum_{l=0}^{L-1}|h[l]|^2}. \tag{9}$$

Subject to the one-tap constraint, the receiver is designed to estimate $X[k-\frac{L-1}{D}]$ solely based on the observation of $Y[k]$. Then, the remaining components of $Y[k]$ can be further categorized into inter-symbol interference (ISI) and noise, as shown in the following

$$\begin{aligned} Y[k] =& \; a(h*g)[L-1]X[k-\frac{L-1}{D}] \quad (Signal) \\ &+ a \sum_{\substack{l=0 \\ l\neq(L-1)/D}}^{(2L-2)/D} (h*g)[Dl]X[k-l] \quad (ISI) \\ &+ an[k] \quad (Noise) \end{aligned} \tag{10}$$

Given a specific realization of the random CIRs, from eqn. (10), one can calculate the signal power P_{Sig} as[2]

$$\begin{aligned} P_{Sig} =& \; E_X\left[\left|(h*g)[L-1]X[k-\frac{L-1}{D}]\right|^2\right] \\ =& \; P\left|(h*g)[L-1]\right|^2 = P\left(\sum_{l=0}^{L-1}|h[l]|^2\right), \end{aligned} \tag{11}$$

where $E_X[\cdot]$ represents the expectation over X. Similarly, the ISI can be derived as

$$\begin{aligned} P_{ISI} =& \; E_X\left[\left|\sum_{\substack{l=0 \\ l\neq(L-1)/D}}^{(2L-2)/D} (h*g)[Dl]X[k-l]\right|^2\right] \\ =& \; P\sum_{\substack{l=0 \\ l\neq(L-1)/D}}^{(2L-2)/D} \left|(h*g)[Dl]\right|^2, \end{aligned} \tag{12}$$

As D increases, the ISI term P_{ISI} will gradually decrease. In the regime where D is such a large positive number that $P_{ISI} \to 0$, we can focus on the signal-to-noise ratio (SNR) only:

$$\mathsf{SNR} = \frac{P_{Sig}}{\sigma^2}. \tag{13}$$

Without using the TR-based transmission, we can express the received signal of direct transmission as

$$Y^{DT}[k] = (X*h)[k] + n[k] = \sum_{l=0}^{L-1} h[l]X[k-l] + n[k], \tag{14}$$

where the superscript "DT" represents "direct transmission", and the AWGN $n[k]$ has a zero mean and a variance σ^2. Using a Rake receiver with L_R fingers, the received signal power[3] can be expressed as [21]

$$P_{Sig}^{DT} = P^{DT}\sum_{l=0}^{L_R-1}|h_{(l)}|^2, \tag{15}$$

where P^{DT} denotes the transmit power of direct transmission, and $h_{(l)}$'s, $l = 0, 1, \cdots, L_R-1$, represent the L_R channel taps with the L_R largest immediate tap gains.

[2]Note that the one-tap gain a does not affect the effective SNR (or SINR), so we consider it as $a = 1$ in the subsequent analysis unless otherwise mentioned.

[3]We assume that rate back-off factor D for direct transmission is also large enough so that the ISI is negligible.

In order for the TR system and the direct transmission to have the same performance, i.e., $\mathsf{SNR}_{TR} = \mathsf{SNR}_{DT}$, we must have

$$P_{Sig} = P_{Sig}^{DT}. \tag{16}$$

Then, we can express the ratio of the transmission power of the two schemes as

$$r_P = \frac{P}{P^{DT}} = \frac{\sum_{l=0}^{L_R-1} |h_{(l)}|^2}{\sum_{l=0}^{L-1} |h[l]|^2}, \tag{17}$$

and the ratio of the expected transmission power needed for TR and direct transmission can be expressed as

$$\tau_P = \frac{E[P]}{E[P^{DT}]} = \frac{E\left[\sum_{l=0}^{L_R-1} |h_{(l)}|^2\right]}{\sum_{l=0}^{L-1} E[|h[l]|^2]}. \tag{18}$$

In order to derive the numerator of (18), one needs to analyze the order statistics of the $|h[l]|^2$'s. However, since the $|h[l]|^2$'s are not identically distributed and it is also unknown which L_R out of all the $|h[l]|^2$'s are the L_R largest channel taps, it is very difficult to obtain the closed-form expression of the numerator in (18). Therefore, we will first assume that the $|h[l]|^2$'s are identically and independently distributed (i.i.d.), and derive the numerator of (18). Then we will calibrate the results for non-identically distributed $|h[l]|^2$'s.

Before we start our analysis, let us first introduce the concept of *quantile* [15] in order statistics. Denote $F(z)$ as the distribution function for a continuous random variable.

Definition 1: Suppose that $F(z)$ is continuous and strictly increasing when $0 < F(z) < 1$. For $0 < q < 1$, the *q-quantile* of $F(z)$ is a number z_q such that $F(z_q) = q$. If F^{-1} represent the inverse of $F(z)$, then $z_q = F^{-1}(q)$.

Now, let us suppose that the $h[l]$'s are i.i.d random variables; then, $|h[l]|^2$ are also i.i.d. Denote $Z_l \triangleq |h[l]|^2$ for short, and the numerator in (18) can be approximated by the sample mean, i.e.,

$$E\left[\sum_{l=0}^{L_R-1} Z_{(l)}\right] \approx \lim_{n\to\infty} \frac{1}{n} \sum_{i=1}^{n} \left[\sum_{l=0}^{L_R-1} z_{(l)}^i\right], \tag{19}$$

where the superscript i denote the i-th trial, and $z_{(0)}^i \geq z_{(1)}^i \geq \cdots \geq z_{(L_R-1)}^i \geq \cdots \geq z_{(L-1)}^i$ represent the ordered descending realization of the Z_l's in the i-th trial.

Since the Z_l's are now supposed to be i.i.d. and the relation between L_R and L generally satisfies $L \gg L_R$, we can further approximate (19) as

$$E\left[\sum_{l=0}^{L_R-1} Z_{(l)}\right] \approx \lim_{n\to\infty} \frac{1}{n} \sum_{l=0}^{nL_R-1} z_{(l)}, \tag{20}$$

where the $z_{(l)}$'s, $l = 0, \cdots, nL_R-1$, represent the nL_R largest realizations among the nL realizations of the random variable Z_l. Since $z_{(nL_R-1)}$, the smallest realization among the $z_{(l)}$'s, $l = 0, \cdots, nL_R-1$, is no less than $nL - nL_R$ out of the total nL realizations, (20) can be approximated as

$$E\left[\sum_{l=0}^{L_R-1} Z_{(l)}\right] \approx L_R E\left[Z_l | Z_l \geq z_{l,q}\right], \tag{21}$$

where $z_{l,q}$ is the q-quantile of Z_l's distribution $F_{Z_l}(z)$, with $q = \frac{nL-nL_R}{nL} = \frac{L-L_R}{L}$.

However, the Z_l's are not identically distributed, so we need to calibrate the results obtained in (21). An upper bound of $E\left[\sum_{l=0}^{L_R-1} |h_{(l)}|^2\right]$ can be obtained by substituting the largest quantile in (21), i.e.,

$$E\left[\sum_{l=0}^{L_R-1} Z_{(l)}\right] \leq L_R E\left[Z_{(0)} | Z_{(0)} \geq z_{(0),q}\right], \tag{22}$$

and an approximation can be expressed as

$$E\left[\sum_{l=0}^{L_R-1} Z_{(l)}\right] \approx \sum_{l=0}^{L_R-1} E\left[Z_{(l)} | Z_{(l)} \geq z_{(l),q}\right], \tag{23}$$

where $z_{(0),q} \geq \cdots \geq z_{(L_R-1),q} \geq \cdots \geq z_{(L-1),q}$, and $Z_{(0)}, \cdots, Z_{(L_R-1)}$ are corresponding random variables.

As defined earlier in Section II, $h[l]$ is a CSCG random variable with $E[|h[l]|^2] = e^{-\frac{lT_s}{\sigma_T}}$. Denote $\sigma_l^2 \triangleq e^{-\frac{lT_s}{\sigma_T}}$, then $\frac{|h[l]|^2}{\sigma_l^2/2} \sim \chi^2(k)$, with $k = 2$. In the special case of $k = 2$, a $\chi^2(k)$ distribution is equivalent to an exponential distribution $\text{Exp}(\lambda)$ with $\lambda = \frac{1}{2}$. After some mathematical derivation, we can get the distribution function of Z_l as

$$F_{Z_l}(z) = \begin{cases} 1 - e^{-\frac{z}{\sigma_l^2}}, z \geq 0, \\ 0, \qquad\quad z < 0. \end{cases} \tag{24}$$

Therefore, Z_l is also exponentially distributed, with mean $E[Z_l] = \sigma_l^2 = e^{-\frac{lT_s}{\sigma_T}}$. Solving the inverse function of $F_{Z_l}(z)$ and substituting $q = \frac{L-L_R}{L}$ yields the q-quantile of Z_l

$$z_{l,q} = -\sigma_l^2 \ln(1-q) = e^{-\frac{lT_s}{\sigma_T}} \ln(\frac{L}{L_R}). \tag{25}$$

Considering the approximation in (23), $z_{(l),q}$ is the $(l+1)$-th largest q-quantile corresponding to $z_{l,q}$ in (25), and $Z_{(l)}$ corresponds to $Z_l \sim \text{Exp}(1/\sigma_l^2)$, we can get

$$E\left[Z_{(l)} | Z_{(l)} \geq z_{(l),q}\right] = \left(1 + \ln\left(\frac{L}{L_R}\right)\right) e^{-\frac{lT_s}{\sigma_T}}. \tag{26}$$

Then, the numerator of (18) can approximated as

$$E\left[\sum_{l=0}^{L_R-1} |h_{(l)}|^2\right] \approx \left(1 + \ln\left(\frac{L}{L_R}\right)\right) \sum_{l=0}^{L_R-1} e^{-\frac{lT_s}{\sigma_T}}, \tag{27}$$

and the upper bound in (22) becomes

$$E\left[\sum_{l=0}^{L_R-1} |h_{(l)}|^2\right] \leq L_R \left(1 + \ln\left(\frac{L}{L_R}\right)\right). \tag{28}$$

Note that for the $|h[l]|^2$'s, $l = 0, 1, \cdots, L-1$, when l is very large, $E[|h[l]|^2] = e^{-\frac{lT_s}{\sigma_T}}$ may become very small if $lT_s \gg \sigma_T$, and the $|h[l]|^2$'s with very small mean values can be negligible compared to those $|h[l]|^2$'s with large mean values. Therefore, to make the upper bound tight and the approximation more precise, we only keep the significant paths whose expected gain is larger than a pre-determined parameter[4] ϵ, i.e., $E[|h[l]|^2] = e^{-\frac{lT_s}{\sigma_T}} \geq \epsilon$. The index of the last significant path is $L_c = \lceil \frac{\sigma_T}{T_s} \ln(\epsilon^{-1}) \rceil$, while the rest paths

[4]Choices of different ϵ values will affect the approximation, e.g., a greater value of ϵ may tighten the upper bound. In this work, we fix $\epsilon = 10^{-3}$, a properly chosen value after trial-and-error, but how to choose a good ϵ is beyond the scope of the paper.

indexed $l = L_c + 1, L_c + 2, \cdots, L - 1$ are neglected in the approximation. Replacing L with L_c in (27) and (28), and substituting them back into (18), we get approximate τ_P as

$$\tau_P \approx \left(1 + \ln\left(\frac{L_c}{L_R}\right)\right) \frac{1 - e^{-L_R T_s/\sigma_T}}{1 - e^{-LT_s/\sigma_T}}, \tag{29}$$

with an upper bounded

$$\tau_P \leq L_R \left(1 + \ln\left(\frac{L_c}{L_R}\right)\right) \frac{1 - e^{-T_s/\sigma_T}}{1 - e^{-LT_s/\sigma_T}}. \tag{30}$$

Since the number of taps of the CIR is in general much greater than the number of fingers of a Rake receiver, we usually have $1 - e^{-L_R T_s/\sigma_T} \ll 1 - e^{-LT_s/\sigma_T}$, and $L_R(1 - e^{-T_s/\sigma_T}) \ll 1 - e^{-LT_s/\sigma_T}$. Thus, the ratio of the power needed for a TR system to achieve the same performance as direct transmission is much less than 1. With a typical number of fingers $L_R = 4$ (for example, 3GPP2 recommends the Rake receiver shall provide a minimum of four fingers for the CDMA 2000 system [16]) and the channel length L = 200, the value of (29) is about 0.1, which implies an order of magnitude reduction in power consumption. According to our experiment and simulation results with typical parameters setting, the energy needed for a TR-based transmission can be as low as 20 % of that needed for a direct transmission with Rake receivers. When the rate back-off factor D is not large, both TR system and the direct transmission face the ISI problem. Although it is difficult to analyze accurately, it has been shown that [19] the temporal focusing effects of TR can significantly reduce the presence of ISI by reducing the channel delay spread. Thus, we expect a similar or even higher level of power reduction can be achieved. Therefore, TR is expected to achieve a much better power efficiency than direct transmission.

B. Interference Alleviation

In this part, we will compare the interference that a transmitter causes to an un-intended receiver using TR-based transmission to that using direct transmission. Assume the CIR between the transmitter to the un-intended victim receiver is

$$h_1[k] = \sum_{l=0}^{L-1} h_{1,l}\delta[k - l], \tag{31}$$

with $h_1[l]$ being the l-th tap of the CIR and L the length of the CIR. Each $h_1[l]$ has the same distribution as $h[l]$, i.e., a circular symmetric complex Gaussian random variable with a zero mean and a variance $e^{\frac{-lT_s}{\sigma_T}}$, but they are assumed to be independent due to the location difference.

Then, we can express the received signal from the transmitter at the victim receiver with the TR-based transmission as

$$\begin{aligned} Y_1[k] = {} & a(h_1 * g)[L-1]X[k - \frac{L-1}{D}] \quad (Signal) \\ & + a \sum_{\substack{l=0 \\ l \neq (L-1)/D}}^{(2L-2)/D} (h_1 * g)[Dl]X[k - l] \quad (ISI) \\ & + an_1[k] \quad (Noise) \end{aligned} \tag{32}$$

For simplicity, we still omit the ISI term by assuming that D is a large positive number, then the interference perceived by the victim receiver is equal to the signal power of $Y_1[k]$, i.e.,

$$I^{TR} = P|(h_1 * g)[L-1]|^2 = P\frac{\left|\sum_{l=0}^{L-1} h_1[l]h^*[l]\right|^2}{\sum_{l=0}^{L-1}|h[l]|^2}. \tag{33}$$

With direct transmission, the received signal perceived by the victim receiver can be written as

$$Y_1^{DT}[k] = (h_1 * X)[k] + n_1[k] = \sum_{l=0}^{L-1} h_1[l]X[k-l] + n_1[k]. \tag{34}$$

Then, the interference at the un-intended receiver can be expressed as

$$I^{DT} = E_X\left[\left|\sum_{l=0}^{L-1} h_1[l]X[k-l]\right|^2\right] = P^{DT}\sum_{l=0}^{L-1}|h_1[l]|^2, \tag{35}$$

and we can obtain the ratio of the interference caused by the two schemes as

$$r_I = \frac{I^{TR}}{I^{DT}}. \tag{36}$$

Define

$$\tau_I = \frac{E[I^{TR}]}{E[I^{DT}]} \tag{37}$$

as the ratio of the expected interference caused by TR and direct transmission. Substituting (33) and (35) into (37) and taking expectation with respect to h and h_1, we can approximate τ_I as

$$\begin{aligned} \tau_I \approx & \tau_P \frac{E\left[\left|\sum_{l=0}^{L-1} h_1[l]h^*[l]\right|^2\right]}{E\left[\left(\sum_{l=0}^{L-1}|h[l]|^2\right)\left(\sum_{l=0}^{L-1}|h_1[l]|^2\right)\right]} \\ = & \tau_P \frac{\sum_{l=0}^{L-1}\left(E\left[|h[l]|^2\right]\right)^2}{E\left[\sum_{l=0}^{L-1}|h[l]|^2\right]\cdot E\left[\sum_{l=0}^{L-1}|h_1[l]|^2\right]} \\ = & \tau_P \frac{\sum_{l=0}^{L-1} e^{-\frac{2lT_s}{\sigma_T}}}{\left(\sum_{l=0}^{L-1} e^{-\frac{lT_s}{\sigma_T}}\right)^2} \\ = & \tau_P \frac{1 + e^{-\frac{LT_s}{\sigma_T}}}{1 - e^{-\frac{LT_s}{\sigma_T}}} \cdot \frac{1 - e^{-\frac{T_s}{\sigma_T}}}{1 + e^{-\frac{T_s}{\sigma_T}}}, \end{aligned} \tag{38}$$

where the second equality holds since $h[l]$ and $h_1[l]$ are i.i.d. random variables, and $h[l]$ and $h_1[k]$ are independent for $l \neq k$. Note that the ratio of the expected transmission power τ_P should be chosen according to (18) in order to maintain the same performance.

In general, the observation time LT_s satisfies $LT_s \gg \sigma_T$, and the sampling period T_S is much smaller than the delay spread σ_T, and thus we know that τ_I is much less than 1. According to our simulation results with typical parameters, under the ideal assumption that channel responses of two different locations are completely independent, interference

could be made 20 dB lower by using the TR-based system. Even for a practical environment where correlation between channel responses does exist, our experiment measurements show that the interference alleviation can be up to 6 dB when the victim receiver is only 1 m away from the intended receiver. Therefore, the interference caused to an un-intended receiver with the TR-based transmission is greatly reduced compared to direct transmission.

C. Multi-Path Gain of TR

Since TR can utilize the multi-paths as virtual multi-antennas, the multiple paths can provide spatial diversity. In this part, we briefly talk about the maximum achievable diversity order of TR transmission.

We first consider a binary phase-shift keying (BPSK) signaling with amplitude $\sqrt{P}$, i.e., $X[k] = \pm\sqrt{P}$. By omitting the ISI term, the error probability of detecting X is

$$Q\left(\sqrt{\frac{P_{Sig}}{\sigma^2/2}}\right) = Q\left(\sqrt{2\left(\sum_{l=0}^{L-1}|h[l]|^2\right)\mathsf{SNR}}\right), \quad (39)$$

where $\mathsf{SNR} = P/\sigma^2$ is the signal-to-noise ratio per symbol time, and $Q(\cdot)$ is the complementary cumulative distribution function of an $N(0,1)$ random variable. By averaging over the random tap gain h and following similar analysis as in [22], we can express the overall error probability as

$$\begin{aligned} p_e &\le \prod_{l=0}^{L-1}\left(1+\mathsf{SNR}\cdot e^{-\frac{lT_s}{\sigma_T}}\right)^{-1} \\ &\le \prod_{l=0}^{L-1}\left(\mathsf{SNR}\cdot e^{-\frac{lT_s}{\sigma_T}}\right)^{-1} \\ &= \left(\prod_{l=0}^{L-1} e^{\frac{lT_s}{\sigma_T}}\right)(\mathsf{SNR})^{-L} \\ &= e^{\frac{L(L-1)T_s}{2\sigma_T}}(\mathsf{SNR})^{-L}. \end{aligned} \quad (40)$$

Thus, the maximum achievable diversity of TR-filtering is L. Similar conclusions can be drawn when other modulation schemes are used, such as quadrature amplitude modulation (QAM) and M-ary phase-shift keying (PSK). For example, if an M-QAM is used, the error probability of a symbol for a fixed channel can be represented by

$$4KQ\left(\sqrt{b_{\mathrm{QAM}}\left(\sum_{l=0}^{L-1}|h[l]|^2\right)\mathsf{SNR}}\right) - 4K^2Q^2\left(\sqrt{b_{\mathrm{QAM}}\left(\sum_{l=0}^{L-1}|h[l]|^2\right)\mathsf{SNR}}\right), \quad (41)$$

where $K = 1 - 1/\sqrt{M}$ and $b_{\mathrm{QAM}} = 3/(M-1)$ [17]. Note that the second term can be dropped because we are interested in the upper bound, and similar derivation can be applied to show that the error probability is asymptotically proportional to $(\mathsf{SNR})^{-L}$.

We have assumed that multi-paths on different channel taps are independent, and there are L independent multi-paths in total, which account for the diversity order of L. In practice, however, it is possible that some multi-path components on nearby channel taps are correlated, and there are possibly some channel taps on which no multi-paths fall in. In that case, we only consider those independent multi-paths, and according to our analysis, the diversity order of a TR system should be equal to the number of independent multi-paths.

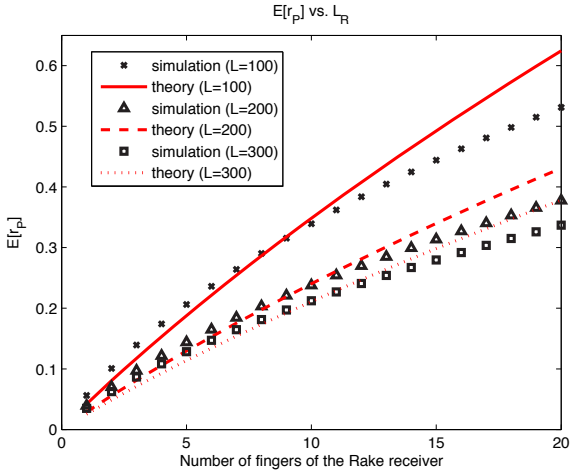

Fig. 3. The expected ratio of energy needed for a TR-based communication system compared with an L_R-finger Rake receiver.

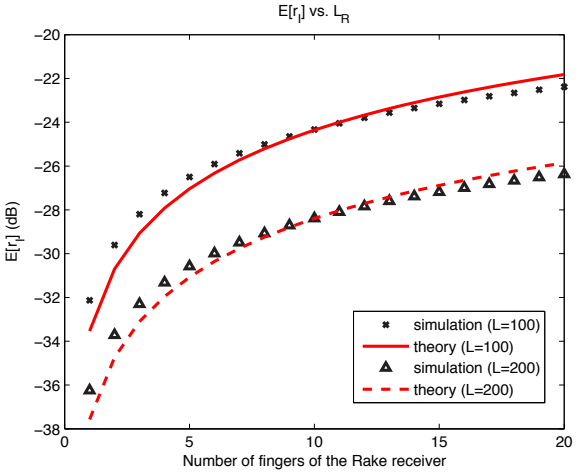

Fig. 4. The expected interference alleviation of a TR-based communication system compared with an L_R-finger Rake receiver.

IV. Simulation Results

In this part, we present some simulation results about the performance of TR transmission, and justify the theoretical results derived in Section III. Simulation results shown in this section are obtained by choosing $\sigma_T = 125T_s$ in the system model. We are interested in the impact of L_R (number of fingers of the Rake receiver) and L (number of channel taps) on the system performance. Because 3GPP2 recommends the Rake receiver shall provide a minimum of four fingers for the CDMA 2000 system [16], and too many fingers may result in unaffordable complexity, we believe comparing the TR-based transmission with a Rake receiver who has four to eight fingers is a relative fair comparison.

In Fig. 3, we compare τ_P approximated in (29) (denoted by "theory") with the value of $E[r_P]$ by averaging r_P over 5000 channel realizations. L_R is varied from 1 to 20, and L is chosen from $\{100, 200, 300\}$. We can see that, as an analytical approximation of $E[r_P]$, τ_P matches simulation results very well in a wide range of L_R ($1 \le L_R < 15$). When there are fewer fingers in the Rake receiver, direct transmission can only get a worse equalization. Thus, in order to have the same receiver performance, direct transmission costs an

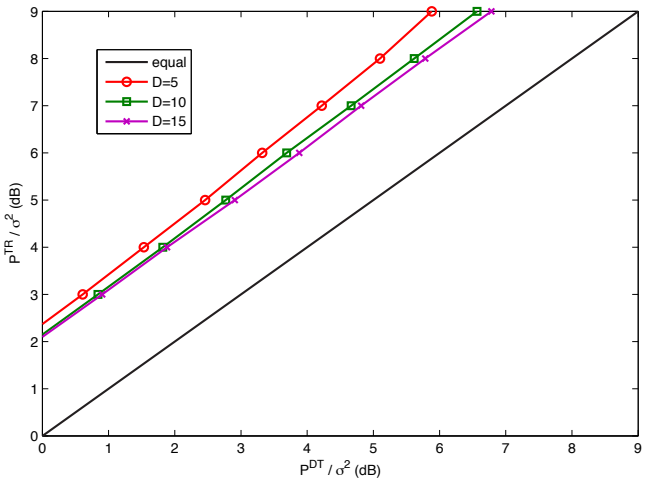

Fig. 5. Expected transmit power needed for a TR-based system vs. an L_R-finger Rake receiver (ISI non-negligible).

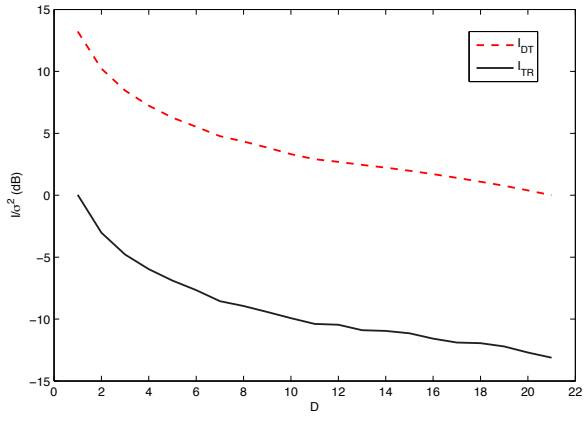

Fig. 6. Expected interference alleviation of a TR-based system vs. an L_R-finger Rake receiver (ISI non-negligible).

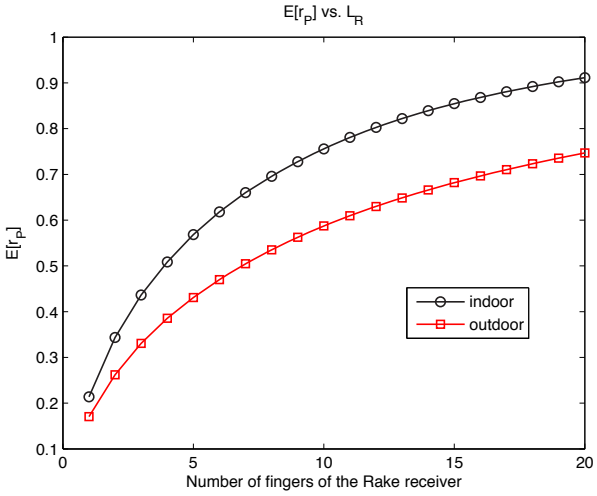

Fig. 7. Expected ratio of energy needed for a TR-based system vs. direct transmission (IEEE 802.15.4a channel model).

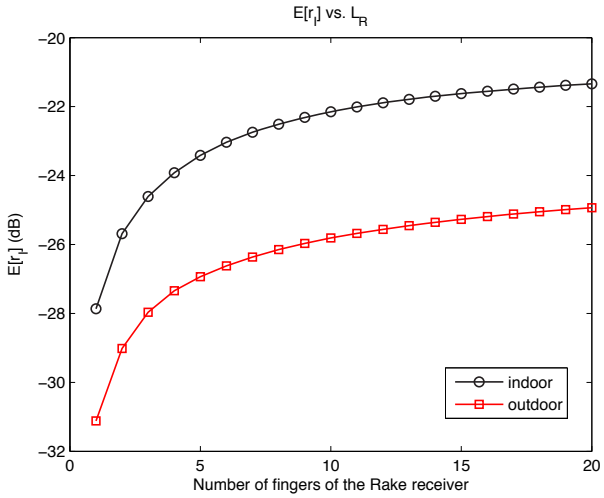

Fig. 8. Expected interference alleviation for a TR-based system vs. direct transmission (IEEE 802.15.4a channel model).

increasing amount of transmission power compared to TR, and TR becomes more energy-efficient than direct transmission, reflected by a decreasing $E[r_P]$. In addition, TR can benefit more from a richer multi-path environment, as shown by the decrease in $E[r_P]$ when L increases from 100 to 300.

In Fig. 4, we compare τ_I with $E[r_I]$ which is obtained by averaging r_I over 5000 realizations. We can see that the τ_I also matches the simulation results $E[r_I]$ very well. Under the system model defined in Section II, the interference caused by TR is 22 dB to 38 dB lower than the interference of direct transmission, depending on different choices of L_R and L. Under a normal parameter setting, e.g., $L = 200$ and $L_R = 6$, the interference of TR is about 30 dB lower, which indicates TR signal transmission can greatly reduce the interference and is thus much "greener".

To simplify the analysis of τ_P and τ_I, we have assumed D is so large that the ISI becomes negligible in Section III. In order to better understand the impact of the parameter D on the transmit power reduction and the interference alleviation, we use simulations to demonstrate $E[r_P]$ and $E[r_I]$ where the ISI cannot be neglected in the received signal for both direct transmission and TR-based transmission. In Fig. 5, we show the ratio between the transmit signal power required by the two schemes against the noise power, in order to achieve the same received SINR performance. For illustration purpose, we choose $L_R = 6$ fingers and $L = 21$ channel taps. The value of factor D is chosen from $\{5, 10, 15\}$ to represent very large, medium, and small ISI, respectively. The blue line with legend "equal" is used to represent the benchmark $P^{DT} = P^{TR}$ for comparing the transmit power of the two schemes. We see from Fig. 5 that in order to achieve the same receiver performance, direct transmission usually requires 2∼3 dB higher transmit power than TR-based transmission. In Fig. 6, we show the interference power comparison when the transmit power of the two schemes follows the relation shown in Fig. 5. We can see that the interference at a victim receiver caused by TR-based transmission is around 13 dB lower than that caused by direct transmission, when D varies in $[1, 21]$. This clearly shows that the capability of power reduction and interference alleviation of TR-based transmission remains even if we want to transmit the signals with a higher data rate, i.e., a smaller D.

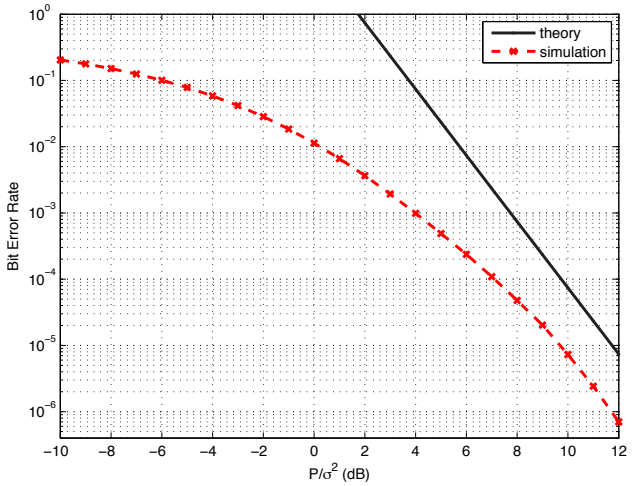

Fig. 9. Illustration of the diversity order using the bit error rate (BER) curve.

In Section II, in order to make the performance analysis tractable, we have assumed a specific channel model as defined in eqn. (2). In order to have a more comprehensive comparison on the performance of TR-based transmission and direct transmission, we also conduct numerical simulations under practical channel models. Although 3GPP channel model is a prevailing channel model, it does not fit in the proposed TR-based scheme, because 3GPP channel models only apply to narrow-band systems, while the TR-based scheme requires a frequency bandwidth of at least several hundred MHz so as to have a plenty of multipath components. As will be seen in the next section, the bandwidth in the experimental measurements actually spans from 490 MHz to 870 MHz. Due to this reason, we chose the IEEE 802.15.4a channel model [23] which is a standard model for wideband transmissions, and simulated both the indoor LOS scenario with L $\sim$ 100 taps and the outdoor NLOS scenario with L $\sim$ 500 taps. The simulation results are shown in Fig. 7 and Fig. 8, where the x-axis denotes the number of fingers of the Rake receiver varying from 1 to 20, and the y-axis denotes the expected power reduction and interference alleviation, respectively. As can be seen from these figures, compared to direct transmission using a 6-finger Rake receiver, TR-based transmission only needs 62% transmit power while reducing the interference by 23 dB in an indoor environment, and for outdoor, TR only needs 48% transmit power while reducing the interference by 27 dB. These clearly show the advantage of TR-based scheme over direct transmission in a practical wireless channel.

Finally, in Fig. 9, we show the multi-path gain of TR, where the channel length is chosen[5] as $L = 5$ and the rate back-off factor is $D = 5$. We can see that in the high SNR regime, the diversity order of TR is around 5, which equals L and thus justifies the derivation in Section III-C.

[5]Although the real channel length is generally much longer than the chosen parameter, computers cannot afford the simulation using real channel length that requires 10^L channel realizations to get an error bit. Therefore, we choose a much shorter multi-path channel just for illustration purpose.

V. Experimental Measurements

In this part, we demonstrate some experimental measurements taken in practical multi-path channels. The tested signal bandwidth spans from 490 MHz to 870 MHz, centered at the carrier frequency 680 MHz. Two measurement sites are considered, an office room and a corridor, both of which are located on the second floor of the J. H. Kim Engineering Building at the University of Maryland. The layout of the two sites are given in Fig. 10, where transceiver *A* transmits time-reversed signals to transceiver *B*, and electromagnetic waves are reflected by walls, ceiling/floor, and other objects in the surrounding area. We fixed the location of transceiver A, whereas moving transceiver B in a rectangular area (the length is about four wave lengths) in the experiment.

A. Channel Impulse Response

In Fig. 11, we show the amplitude of the channel impulse response (CIR) in the two tested sites. Due to the plentiful reflections by the walls of the small room, there are more paths (larger delay spread) for the office environment than in the corridor. Moreover, the amplitude also decays more slowly in the office environment, since the signal waveforms are bounced back and forth and thus last longer in time. In Fig. 11(c), we show the normalized magnitude of the received signals using the TR transmission in the corridor. We see clearly that TR can compress a substantial portion of signal power into very few taps, i.e., has the temporal focusing effect.

B. Power Reduction

Due to the temporal focusing effect, TR can utilize the multi-paths as multiple antennas to harvest energy from the environment. By varying the number of fingers of a Rake receiver for direct transmission, we show the ratio of the transmission power of a TR system over direct transmission in Fig. 12. We can see that in order to achieve the same receiver performance, TR only costs as low as 30 % of the transmission power of direct transmission, given that a Rake receiver usually has less ten fingers, for both the office and the corridor. When the Rake receiver has six fingers, the ratio of power reduces to 20 % for the office and 24 % for the corridor. This shows that TR can achieve highly energy-efficient communication without requiring much complexity for the transmitter and the receiver. It is worth noting that the experimental measurement shown here in Fig. 12 has a similar trend as the case of $L = 200$ in Fig. 3.

C. Interference Alleviation

Besides energy-efficiency due to the temporal focusing effect, the time-reversed waves can also retrace the incoming paths, resulting in a spiky spatial signal power distribution focused at the intended receiver. This indicates by using TR, a transmitter will cause little interference to an un-intended receiver. In this part, we demonstrate the spacial focusing effect of TR and the resulting interference alleviation. In the experiment, we used the time-reversed CIR associated with the intended receiver as a basic waveform to load data streams, and moved the receive antenna by a step size of $\lambda/2$,

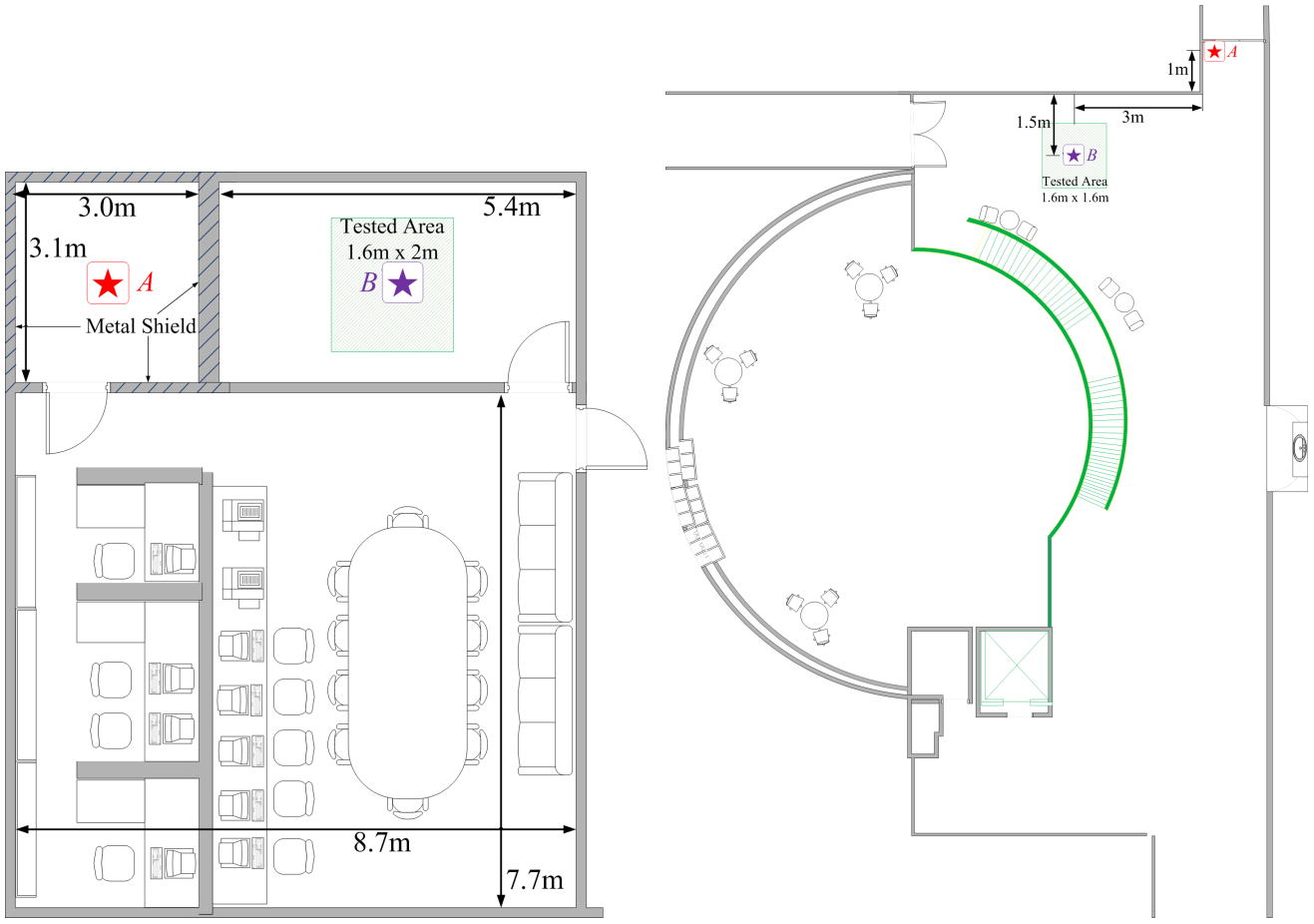

(a) Layout of the office site

(b) Layout of the corridor site

Fig. 10. Floor plan and the layout of the test sites.

where λ is the wave length corresponding to carrier frequency 680 MHz.

The received signal power distribution (normalized by the peak power) in the spatial domain is shown in Fig. 13. We see that the spike is centered at the intended receiver located at point $(6, 6)$ for office measurements and $(4, 4)$ for corridor measurements, whereas the received signal power in the other locations is only 20 % to 30 % of the signal power in the intended location. Therefore, it is highly possible that the interference leakage caused by a transmitter using the TR-based transmission will be much smaller than that without using TR. We show the interference ratio r_I between TR and direct transmission in Fig. 14, assuming that the power ratio r_P corresponds to a six-finger Rake receiver. We can see that on average the interference caused by TR transmission is 3 dB lower than the interference of direct transmission.

One may notice that the interference alleviation shown here is not as good as that shown in Fig. 4. The reason is that our system model assumes ideal channel independence among different transmission pairs, e.g., when they are very far apart in space. Thus, the interference shown by the simulation results is much lower than the results obtained by measurements, where the channels are actually not perfectly independent but correlated. However, as shown in Fig. 14, when the un-intended receiver is 2λ (less than 1 m in our experiment) away from the intended receiver, the least interference caused by TR transmission can be as low as 6 dB lower, and we can expect even less severe interference when the un-intended receiver is farther away. This result demonstrates that TR transmission has a high resolution of spatial selectivity and low pollution to the surrounding environment, which makes it a perfect candidate paradigm for future green wireless communications.

Furthermore, we can observe that the corridor site has better interference alleviation results than the office site. Because the office is a more enclosed environment where waves resonate between walls and lots of objects, the energy dissipates much slower and the interference is relatively high. Hence, we can expect further reduction in interference if the communications take place in the outdoor environment which is an open space.

D. Spectral Efficiency

A prerequisite of TR transmission is that the transmitter needs to use the time-reversed channel response as the basic waveform to load data. If the channel is fast fading, then the receiver needs to continuously transmit short pilot pulses to the transmitter so that the transmitter can get immediate CIR. In the worst case, the receiver needs to send pilot pulses before every transmission attempt of the transmitter, leading to a spectral efficiency of 50 %. In this part, we use experiment results to show that the multi-path channel of an office environment is actually not changing a lot. In

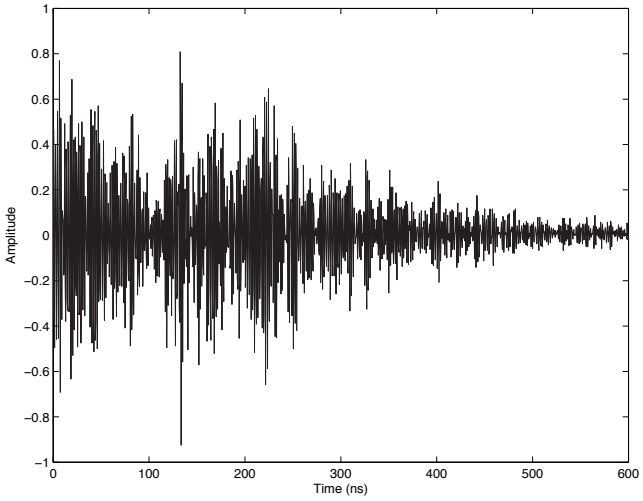

(a) CIR (office)

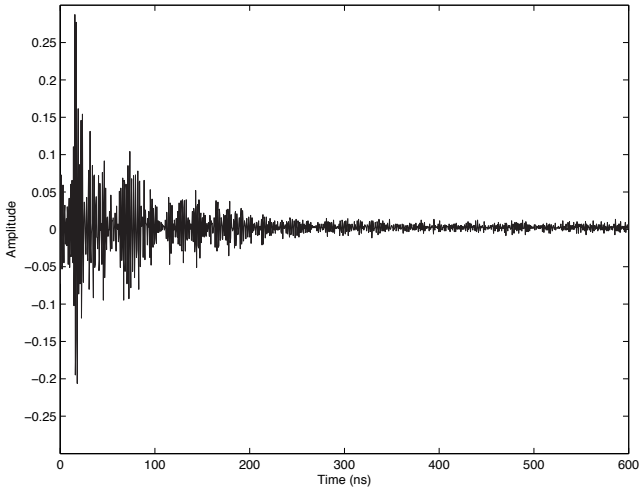

(b) CIR (corridor)

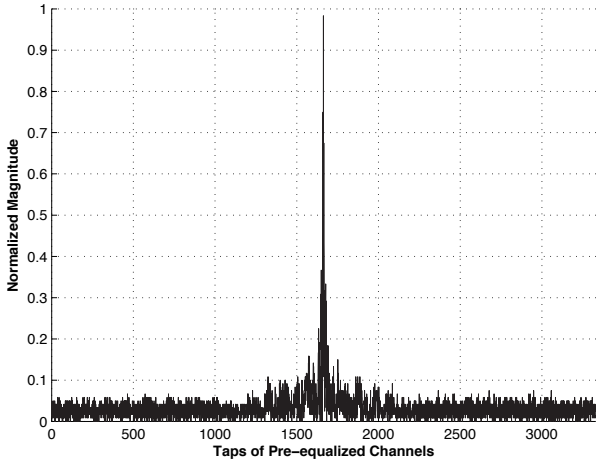

(c) Temporal focusing effect (corridor)

Fig. 11. Channel impulse responses and temporal focusing effect obtained from experiments.

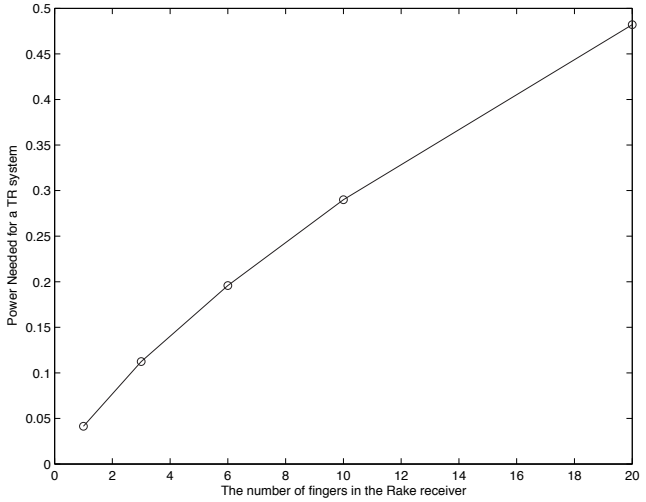

(a) r_P (office)

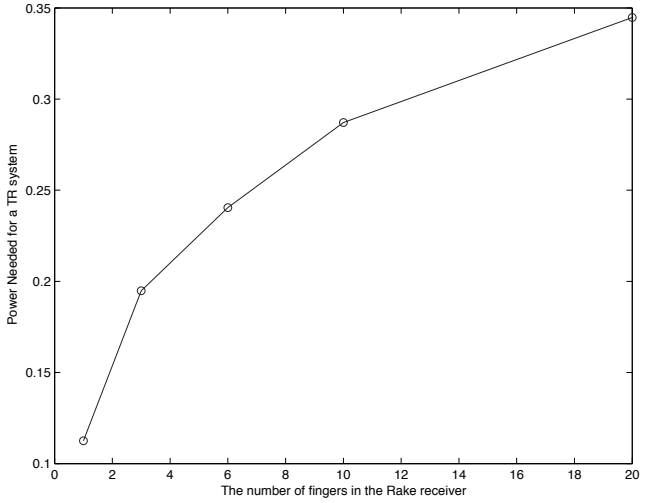

(b) r_P (corridor)

Fig. 12. Power reduction by the TR-based transmission obtained by the experiment measurements.

this experiment, we measured the channel every one minute, and a total of 40 channel snapshots were taken and stored. In the first twenty minutes, the testing environment was kept static; in the following ten minutes, one experimenter walked randomly around the receive antenna (about 1.5 m–3 m away); in the last ten minutes, the experimenter walked very close to the antenna (within 1.5 m). In other words, snapshots 1–20 correspond to a static environment, snapshots 21–30 correspond to a moderately varying environment, and snapshot 31–40 correspond to a varying environment.

We calculated the correlation coefficient between different snapshots to gain an idea of how the channel impulse response varies. Fig. 15 illustrates the correlation matrix for this experiment, where each grid represents the correlation between two snapshots, whose indices are given by the x- and y- coordinates. Most correlation coefficients between static snapshots (1 to 20) are above 0.95, which implies that the channel responses are strongly correlated when the testing environment is static. When the experimenter moved around the antenna, some rays might be blocked and additional reflection paths might be introduced. Therefore, the channel response will vary from its baseline, i.e., the static response. From our experiment, although the correlation drops when there are human activities near the antenna (snapshot 21–30) and becomes even weaker when the experimenter is very

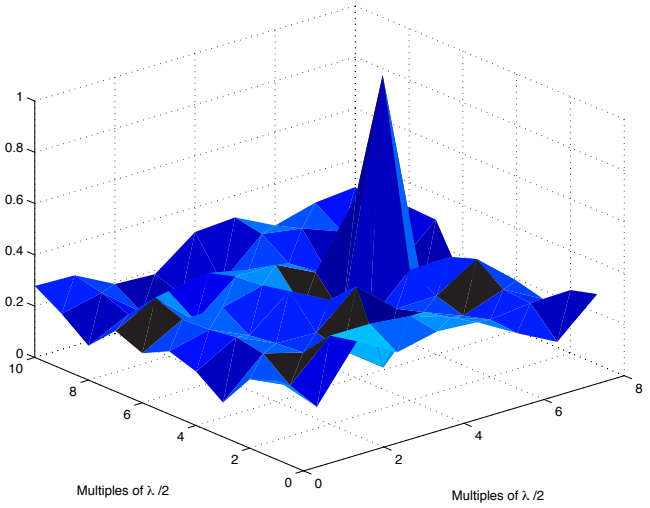

(a) Received signal power (office)

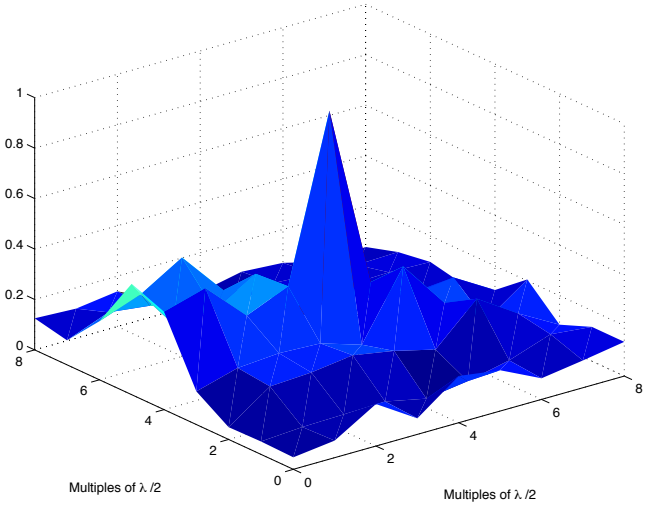

(b) Received signal power (corridor)

Fig. 13. Spatial focusing effect of the TR-based transmission from the experiment measurements.

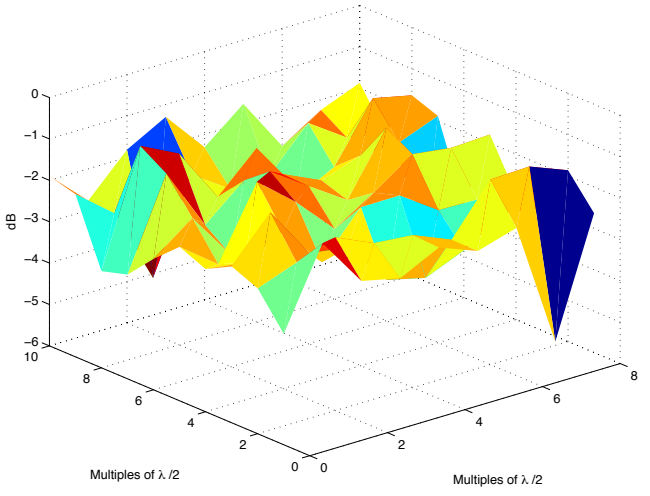

(a) r_I (office)

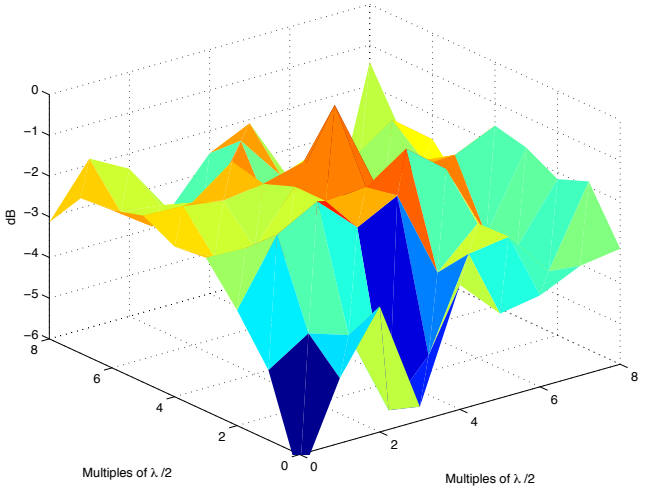

(b) r_I (corridor)

Fig. 14. Interference alleviation by the TR-based transmission obtained by the experiment measurements.

close to the antenna (snapshot 31–40), most of the coefficients are still higher than 0.8. This suggests that good correlation is maintained even if the environment is varying, and the achievable spectral efficiency will be much higher than 50 %.

VI. Time-Reversal Division Multiplexing and Security

Due to its special features and focusing effect, the TR-based communications will spark a series of unique wireless applications, in addition to the low-power low-interference green communications. In this section, we briefly introduce two prospective applications based on the TR communication technology.

A. Time-Reversal Division Multiplexing

In a multi-user system, different users have to find a way to share the wireless media. Traditional approaches include time division multiplexing (TDM), frequency division multiplexing (FDM), and code division multiplexing (CDM). The recent advance in multi-input multi-output (MIMO) has brought in a new multiplexing scheme named spatial division multiplexing (SDM), where different users can be distinguished by their channel response vectors due to the equipment of multiple antennas. In a rich scattering environment, since different users have different unique multi-path profiles which depend on their physical locations and TR transmission treats each path like a virtual antenna, it is possible to utilize multi-path profiles as a way to distinguish different users, which may facilitate the multiplexing. Therefore, a new TR-based multiplexing scheme, time-reversal division multiplexing (TRDM), for a multiuser downlink system can be developed [18].

The TRDM exploits the nature of the multi-path environment, utilizes the location-specific signatures between the base station and multiple users to separate intended signals, and thus achieves satisfying performance. Furthermore, the TRDM approach will make possible numerous applications that require accurately locating the receiver, e.g., automatic inventory management in a warehouse, and wireless mailbox where a server could deliver information to a specific office in a building.

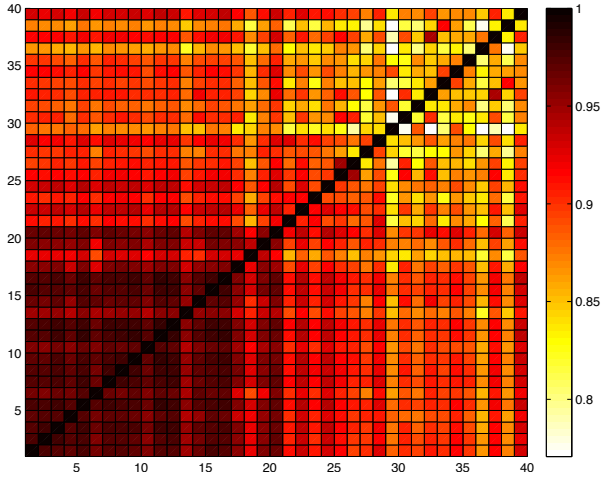

Fig. 15. Correlation of channel responses at different time epochs.

B. Time-Reversal Based Security

Secret communications have been of critical interest for quite a long time. Because of the fast technology evolution, a malicious attacker may easily find some low-cost radio equipments or easily modify the existing equipments to enable a potential intrusion. Moreover, wireless networks are extremely vulnerable to malicious attacks due to the broadcasting nature of wireless transmission and often a distributed network structure. As a result, traditional security measures may become insufficient to protect wireless networks. Therefore, TR-based communications can be exploited to enhance system security based on the unique location-specific multi-path profile.

In a rich scattering wireless environment, multiple paths are formed by numerous surrounding reflectors. For receivers at different locations, the received waveforms undergo different reflecting paths and delays, and hence the multi-path profile can be viewed as a *unique location-specific signature*. As this information is only available to the transmitter and the intended receiver, it is very difficult for other unauthorized users to infer or forge such a signature. It has been shown in [20] that even when the eavesdroppers are close to the target receiver, the received signal strength is much lower at the eavesdroppers than at the target receiver in an indoor application, because the received signals are added incoherently at the eavesdroppers. The security based on multi-path profiles is two-fold: first, the multi-path profile can be used to derive a symmetric key for the transmitter-receiver pair, which protects the secret information from malicious users; second, the transmitter can employ the TR-based transmission to hide the information from eavesdroppers, thanks to the spatial focusing effect.

The scheme is somehow like the direct sequence spread spectrum (DSSS) based secret communications. In DSSS communications, the energy of an original data stream is spread to a much wide spectrum band by using a pseudo-random sequence, and the signal is hidden below the noise floor. It is only those who know the pseudo-random sequence that could recover the original sequence from the noise-like signals. However, if the pseudo-random sequence has been leaked to a malicious user, that user is also capable of decoding the secret message. Nevertheless, for our proposed TR-based security, this would no longer be a problem, because the underlying spreading sequence is not a fixed choice but instead a location-specific signature. For the intended receiver, the multi-path channel automatically serves as a decipher that recovers the original data sent by the transmitter; and for all other ineligible users at different locations, the signal that propagates to their receivers would be noise-like and probably is hidden below the noise floor. Therefore, malicious users are unable to recover the secret message, because the security is inherent in the physical layer.

VII. Conclusion

In this paper, we argue and show that TR-based transmission system is an ideal candidate for green wireless communications. By receiving pilot pulses from the receiver and sending back the reversed waveforms, the transmitter can focus energy at the receiver in both spatial and temporal domains with high resolution, and thus harvest energy from the environment and cause less interference to other receivers. We have investigated the system performance, including power reduction, interference alleviation, and multi-path diversity gain. The results show that the TR system has a potential of over an order of magnitude of reduction in power consumption and interference alleviation, as well as a very high multi-path diversity gain. Both numerical simulations and experimental measurements have shown that TR-based transmission can greatly reduce transmission power consumption and inter-user interference. Moreover, strong channel correlation is also demonstrated, showing that TR can achieve green wireless communication with high spectral efficiency even in a time-varying environment.

Acknowledgment

The authors would like to thank Ziva Corporation and David Smith for the use of the radio experiment testbed developed in a prior joint DARPA project.

References

[1] M. Fink, C. Prada, F. Wu, and D. Cassereau, "Self focusing in inhomogeneous media with time reversal acoustic mirrors," *IEEE Ultrasonics Symposium*, vol. 1., pp. 681-686, 1989.

[2] C. Prada, F. Wu, and M. Fink, "The iterative time reversal mirror: A solution to self-focusing in the pulse echo mode," *J. Acoustic Society of America*, vol. 90, pp. 1119-1129, 1991.

[3] M. Fink, "Time reversal of ultrasonic fields. Part I: Basic principles," *IEEE Trans. Ultrason., Ferroelectr., Freq. Control*, vol. 39, no. 5, pp. 555-566, September 1992.

[4] C. Dorme and M. Fink, "Focusing in transmit-receive mode through inhomogeneous media: The time reversal matched filter approach," *J. Acoustic Society of America*, vol. 98, no. 2, part.1, pp. 1155-1162, August 1995.

[5] W. A. Kuperman, W. S. Hodgkiss, and H. C. Song, "Phase conjugation in the ocean: Experimental demonstration of an acoustic time-reversal mirror," *J. Acoustic Society of America*, vol. 103, no. 1, pp. 25-40, January 1998.

[6] H. C. Song, W. A. Kuperman, W. S. Hodgkiss, T. Akal, and C. Ferla, "Iterative time reversal in the ocean," *J. Acoustic Society of America*, vol. 105, no. 6, pp. 3176-3184, June 1999.

[7] D. Rouseff, D.R. Jackson, W. L. Fox, C. D. Jones, J. A. Ritcey, and D. R. Dowling, "Underwater acoustic communication by passive-phase conjugation: theory and experimental results," *IEEE J. Ocean. Eng.*, vol. 26, pp. 821–831, 2001.

[8] B. E. Henty and D. D. Stancil, "Multipath enabled super-resolution for RF and microwave communication using phase-conjugate arrays," *Physical Review Letters*, vol. 93, no. 24, pp. 243904(4), December 2004.
[9] G. Lerosey, J. de Rosny, A. Tourin, A. Derode, G. Montaldo, and M. Fink, "Time reversal of electromagnetic waves," *Physical Review Letters*, vol. 92, pp. 193904(3), May 2004.
[10] M. Emami, M. Vu, J. Hansen, A. J. Paulraj, and G. Papanicolaou, "Matched filtering with rate back-off for low complexity communications in very large delay spread channels," *Proc. 38th Asilomar Conf. Signals, Syst. Comput.*, vol. 1, pp. 218–222, Nov. 2004.
[11] Y. Jin and J. M. F. Moura, "Time reversal imaging by adaptive interference canceling," *IEEE Trans. Signal Process.*, vol. 56, no. 1, pp. 233-247, January 2008.
[12] J. M. F. Moura and Y. Jin, "Detection by time reversal: single antenna," *IEEE Trans. Signal Process.*, vol. 55, no. 1, pp. 187–201, 2007.
[13] Y. Jin and J. M. F. Moura, "Time reversal detection using antenna arrays," *IEEE Trans. Signal Process.*, vol. 57, no. 4, pp. 1396–1414, April 2009.
[14] A. J. Goldsmith, *Wireless Communication*, 1st Ed., New York: Cambridge University, 2005.
[15] A. M. Law, *Simulation Modeling and Analysis*, 4th Ed., McGraw-Hill New York, 2007.
[16] 3GPP2, *Physical Layer Standard for CDMA2000 Spread Spectrum Systems*, Rev-E, June 2010.
[17] M. K. Simon and M. S. Alouini, "A unified approach to the performance analysis of digital communication over generalized fading channels," *Proc. IEEE*, vol. 86, no. 9, pp. 1860–1877, Sept. 1998.
[18] F. Han, Y. H. Yang, B. Wang, Y. Wu, and K. J. R. Liu, "Time-reversal division multiplexing in multi-path channels," *IEEE Conference on Communications (ICC)* 2011, submitted.
[19] P. Blomgren, P. Kyritsi, A. Kim, and G. Papanicolaou, "Spatial focusing and intersymbol interference in multiple-input-single-output time reversal communication systems," *IEEE J. Ocean. Eng.*, vol. 33, no. 3, pp.341-355, July 2008.
[20] X. Zhou, P. Eggers, P. Kyritsi, J. Andersen, G. Pedersen, and J. Nilsen, "Spatial focusing and interference reduction using MISO time reversal in an indoor application," *IEEE Workshop on Statistical Signal Processing (SSP 2007)*, pp. 307-311.
[21] Kyungwhoon Cheun, "Performance of direct-sequence spread-spectrum RAKE receivers with random spreading sequences," *IEEE Trans. Commun.*, vol. 45, no. 9, pp. 1130-1143, Sep. 1997.
[22] D. Tse and P. Viswanath, *Fundamentals of Wireless Communication*, Cambridge University Press, 2005.
[23] A. F. Molisch, B. Kannan, D. Cassioli, C. C. Chong, S. Emami, A. Fort, J. Karedal, J. Kunisch, H. Schantz, U. Schuster and K. Siwiak, "IEEE 802.15.4a channel model - final report", *IEEE 802.15-04-0662-00-004a*, San Antonio, TX, USA, Nov. 2004.

Beibei Wang (S'07-M'11) received the B.S. degree in electrical engineering (with the highest honor) from the University of Science and Technology of China, Hefei, in 2004, and the Ph.D. degree in electrical engineering from the University of Maryland, College Park in 2009. From 2009 to 2010, she was a research associate at the University of Maryland. Currently, she is a senior engineer with Corporate Research and Development, Qualcomm Incorporated, San Diego, CA.

Her research interests include wireless communications and networking, including cognitive radios, dynamic spectrum allocation and management, network security, and multimedia communications. Dr. Wang was the recipient of the Graduate School Fellowship, the Future Faculty Fellowship, and the Dean's Doctoral Research Award from the University of Maryland, College Park. She is a coauthor of *Cognitive Radio Networking and Security: A Game-Theoretic View*, Cambridge University Press, 2010.

Yongle Wu (S'08) received the Ph.D. degree in Electrical and Computer Engineering from University of Maryland, College Park in 2010. He received the B.S. (with highest honor) and M.S. degrees in Electronic Engineering from Tsinghua University, Beijing, China, in 2003 and 2006, respectively. He is currently a senior engineer with Qualcomm Incorporated, San Diego, CA.

His research interests are in the areas of wireless communications and networks, including cognitive radio techniques, dynamic spectrum access, network security, and MIMO-OFDM communication systems. Mr. Wu received the Graduate School Fellowship from the University of Maryland in 2006, the Future Faculty Fellowship in 2009 and the Litton Industries Fellowship in 2010, both from A. James Clark School of Engineering, University of Maryland, and the Distinguished Dissertation Fellowship from Department of Electrical and Computer Engineering, University of Maryland in 2011.

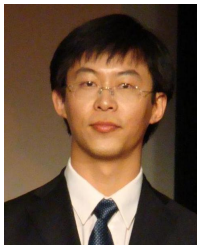

Feng Han (S'08) received the B.S. and M.S. degrees in Electronic Engineering from Tsinghua University, Beijing, China, in 2007 and 2009, respectively. He is currently pursuing the Ph. D. degree in Electrical Engineering, at the University of Maryland, College Park. His current research interests include wireless communications and networking, smart grid, game theory, and information theory.

He is a recipient of the first prize in the 19th Chinese Mathematical Olympiad, the Best Thesis Award of Tsinghua University, the honor of Excellent Graduate of Tsinghua University, and the A. James Clark School of Engineering Distinguished Graduate Fellowship from the University of Maryland, College Park. He received a Best Paper Award for his work on MIMO system at IEEE WCNC'08, Las Vegas, NV, in 2008.

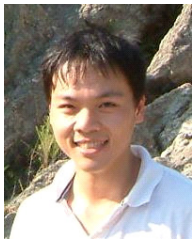

Yu-Han Yang (S'06) received his B.S. in electrical engineering in 2004, and two M.S. degrees in computer science and communication engineering in 2007, from National Taiwan University, Taipei, Taiwan. He is currently pursuing the Ph.D. degree at the University of Maryland, College Park. His research interests include wireless communication and signal processing. He received Class A Scholarship from National Taiwan University in Fall 2005 and Spring 2006. He is a recipient of Study Abroad Scholarship from Taiwan (R.O.C.) Government in 2009 and 2010.

K. J. Ray Liu (F'03) is named a Distinguished Scholar-Teacher of University of Maryland, College Park, in 2007, where he is Christine Kim Eminent Professor of Information Technology. He serves as Associate Chair of Graduate Studies and Research of Electrical and Computer Engineering Department and leads the Maryland Signals and Information Group conducting research encompassing broad aspects of wireless communications and networking, information forensics and security, multimedia signal processing, and biomedical engineering.

Dr. Liu is the recipient of numerous honors and awards including IEEE Signal Processing Society Technical Achievement Award and Distinguished Lecturer. He also received various teaching and research recognitions from University of Maryland including university-level Invention of the Year Award; and Poole and Kent Senior Faculty Teaching Award and Outstanding Faculty Research Award, both from A. James Clark School of Engineering. An ISI Highly Cited Author in Computer Science, Dr. Liu is a Fellow of IEEE and AAAS.

Dr. Liu is President-Elect and was Vice President - Publications of IEEE Signal Processing Society. He was the Editor-in-Chief of IEEE Signal Processing Magazine and the founding Editor-in-Chief of EURASIP Journal on Advances in Signal Processing.